in patients with Brugada syndrome: Using bodysurface signal-averaged electrocardiography and body surface maps. J Cardiovasc Electrophysiol 2004; 15:870–876.

31. Izumida N, Asano Y, Doi S, et al. Changes in body surface potential distributions induced by isoproterenol and Na channel blockers in patients with the Brugada syndrome. Int J Cardiol 2004; 95:261–268.

32. Haws CW, Lux RL. Correlation between in vivo transmembrane action potential durations and activation-recovery intervals from electrograms: Effects of interventions that alter repolarization time. Circulation 1990; 81:281–288.

33. Coronel R, Casini S, Koopmann TT, et al. Right ventricular fibrosis and conduction delay in a patient with clinical signs of Brugada syndrome: A combined electrophysiological, genetic, histopathologic, and computational study. Circulation 2005; 112:2769–2777.

34. Frustaci A, Priori SG, Pieroni M, et al. Cardiac histological substrate in patients with clinical phenotype of Brugada syndrome. Circulation 2005; 112:3680–3687.

35. Aiba T, Shimizu W, Hidaka I, et al. Cellular basis for trigger and maintenance of ventricular fibrillation in the Brugada syndrome model: High resolution optical mapping study. J Am Coll Cardiol 2006; 47:2074–2085.

Magnetocardiography Study on Ventricular Depolarization-Current Pattern in Patients with Brugada Syndrome and Complete Right-Bundle Branch Blocks

AKIHIKO KANDORI, Ph.D.,* TSUYOSHI MIYASHITA, M.S.,* KUNIOMI OGATA, M.S.,* WATARU SHIMIZU, M.D., Ph.D.,† MIKI YOKOKAWA, M.D.,† SHIRO KAMAKURA, M.D., Ph.D.,† KUNIO MIYATAKE, M.D., Ph.D.,† KEIJI TSUKADA, Ph.D.,‡ SATSUKI YAMADA, M.D., Ph.D.,£ SHIGEYUKI WATANABE, M.D., Ph.D.,§ and IWAO YAMAGUCHI, M.D., Ph.D.§

From the *Advanced Research Laboratory, Hitachi, Ltd., 1-280 Higashi-Koigakubo, Kokubunji, Tokyo 185-8601, Japan, †National Cardiovascular Center, Osaka, Japan, ‡Department of Electrical and Electronic Engineering, Okayama University, Okayama, Japan, £Mayo Clinic, Rochester, Minnesota, USA, and §Tsukuba University, Tsukuba, Ibaraki, Japan

Background: *The objective of this study is to use magnetocardiography to determine the existence of a small abnormal current during ventricular depolarization in patients with Brugada syndrome. To understand this small difference in abnormal current during ventricular depolarization, we compared abnormal currents of patients with cases of complete right-bundle-branch block (CRBBB).*

Methods and Results: *We developed a whole-heart electrical bull's eye map (WHEBEM) that uses magnetocardiograms (MCGs) to visualize the current distribution in a circular map. MCGs of Brugada syndrome patients (n = 16), CRBBB patients (n = 10), and controls (n = 12) at rest were recorded. In the WHEBEMs of Brugada syndrome patients, the magnitude of the S-wave current in the upper-right direction of the anterior side is larger than that of the controls. In addition, the R-wave current direction is similar to that of the controls, and the R-wave vector is distributed over a larger area than that of the controls. On the other hand, the CRBBB patients have a distribution of R-wave currents over a larger area in the left anteromedian region and the left posteromedian region. Moreover, in all CRBBB patients, S-wave currents with a large magnitude have the same direction distributed over a small area.*

Conclusions: *The WHEBEM findings suggest that there is an abnormal current in the direction to the upper right (in the S-wave) in the anterosuperior region of Brugada syndrome patients. We thus conclude that a WHEBEM has the potential to detect characteristics of heart disease. (PACE 2006; 29:1359–1367)*

Brugada syndrome, right-bundle-branch block, depolarization, arrhythmia, magnetocardiogram

Introduction

Since the first report by Brugada and Brugada in 1992,[1] the Brugada syndrome has been studied by electrocardiogram (ECG).[2-9] Brugada syndrome is characterized by a unique abnormality pattern in an ECG, indicating frequently atypical, pseudo incomplete right-bundle-branch block (IRBBB) or complete right-bundle-branch block (CRBBB) associated with ST-segment elevation in the right precordial leads (V_1-V_2)[1-7] or in the anteroseptal wall (V_1-V_3).[10] Heterogeneity in repolarization across the ventricular wall of the right-ventricular outflow tract (RVOT) may be the cause of the ST elevation and ventricular tachycardia/ventricular fibrillation (VT/VF).[11]

A magnetocardiogram (MCG) visualizes a pseudo-current distribution in the heart because tangential components of the magnetic field (or a tangential vector calculated from the normal component of a magnetic field) exhibit a pattern of peaks immediately above an electrically activated region due to little interference by various organs such as the lungs and bones.[12,13] Therefore, many clinical applications using these merits of MCG have been published, and literature about MCG has been reviewed.[14,15] In particular, the MCG visualization technique has provided a high detection rate of abnormalities to diagnose adult ischemic and arrhythmic heart diseases.[9]

To observe the occurrence of the abnormal current due to ST elevation, we have used MCG,[16,17] which visualizes current distributions with a high spatial resolution.[9] As a result, we found that an abnormal current at the time of the ST elevation appears in the RVOT,[11] and there is a difference in the spatial conduction pathway during the depolarization.[17] The observation of depolarization abnormality is very important in understanding the mechanism of right-ventricle conduction delay[18]

and VT/VF initiation.[11] In particular, questions regarding the abnormality of the S- and R-wave currents remain.

To distinguish the abnormality, we used a whole-heart electrical bull's eye map (WHEBEM) that we developed, which visualizes the current distribution in a circular map. By comparing WHEBEMs of Brugada syndrome and CRBBB patients, we can understand the depolarization abnormality of a small electrical variance.

Methods

Subjects

We studied 16 Brugada syndrome patients (male/female: 15/1; age: 44±18-year old), 10 CRBBB patients (male/female: 6/4; age: 60±17-year old), and 12 normal control subjects (male/female: 5/7; age: 31±7-year old). In the Brugada syndrome patients, seven patients had asymptomatic Brugada syndrome, while the others had symptomatic Brugada syndrome. Furthermore, two patients had Brugada syndrome with CRBBB and one patient had Brugada syndrome with IRBBB. The normal control group had normal ECGs as well as a clinical history of normal physical examinations. These subjects were measured at two hospitals (the National Cardiovascular Center and Tsukuba University Hospital). The diagnosis of Brugada syndrome was based on typical ECG patterns (i.e., persistent or transient right-precordial ST-segment elevation on right precordial leads or the anteroseptal wall with or without an atypical right-bundle-branch block) and clinical arrhythmic events (syncope, VF, or cardiac arrest).

Magnetocardiogram Recordings and Setup

MCG signals covering the anterior and posterior planes above the chest from each subject were recorded in a resting state over a period of 30 minutes. These signals were detected by a magnetocardiography system (Hitachi, Ltd., Tokyo, Japan)[9] in a magnetically shielded room. They were passed through an analog bandpass filter (0.1–100 Hz) and an analog notch filter (50 Hz). After that, they were digitized at a sampling rate of 1 kHz by an analog-digital converter mounted in a PC. To remove the noise in the signals, the MCG data were averaged using ECG signals as a trigger. All the resulting averaged MCG waveforms were drawn in one trace to visualize the timing of the P-waves, QRS-complexes, and T-waves.

Method of Constructing WHEBEM

A WHEBEM is produced in four calculation steps. First, two MCG measurements (anterior and posterior) are converted to a current arrow map (CAM). The MCG system produces a CAM indicated by pseudo currents (Ix and Iy) from the derivatives of the normal component (Bz) of the MCG signals:

$$Ix = dBz/dy \quad (1)$$

and

$$Iy = -dBz/dx. \quad (2)$$

The magnitude of the current arrows ($I = (Ix^2 + Iy^2)^{1/2}$) is plotted as a contour map. The CAM helps us to understand spatial electrical activity of the heart.[9]

Second, the measurement axes of the anterior and posterior sides are converted to polar coordinates, as shown in Figure 1. Third, the minimum square-root method is used to calculate a weight parameter for adjusting the magnitude of the two (anterior and posterior) converted current arrows because these magnitudes depend on the distance from the heart. The weight parameters (α) are calculated by minimizing the cost function as follows:

$$F(\alpha) = \sum_{t=1}^{T} \sum_{i=1}^{8} \{(A1(i, t) - \alpha A2(i, t))^2 \\ + (B1(i, t) - \alpha B2(i, t))^2, \quad (3)$$

where A1 and A2 indicate anterior and posterior CAM on the right, B1 and B2 indicate anterior and posterior CAM on the left side.

Finally, the converted current arrows are combined by using a connecting interpolation area (A3 and B3) to obtain a WHEBEM. The CAMs of A3 and B3 are calculated as follows:

$$A3(i, t) = \frac{A1(i, t) + \alpha A2(i, t)}{2} \quad (4)$$

and

$$B3(i, t) = \frac{B1(i, t) + \alpha B2(i, t)}{2}. \quad (5)$$

The obtained WHEBEM enables visualization of the current distribution.

WHEBEM can be interpreted as follows:

1. The center of the WHEBEM is the septum of the heart,
2. The bottom of the WHEBEM indicates the posterior of the heart, and the top of the WHEBEM indicates the anterior of the heart,
3. The red contour position indicates the strongest activated area, and
4. Arrows in the red contour indicate the direction of current flows, where

The color indicates the magnitude of the CAM.
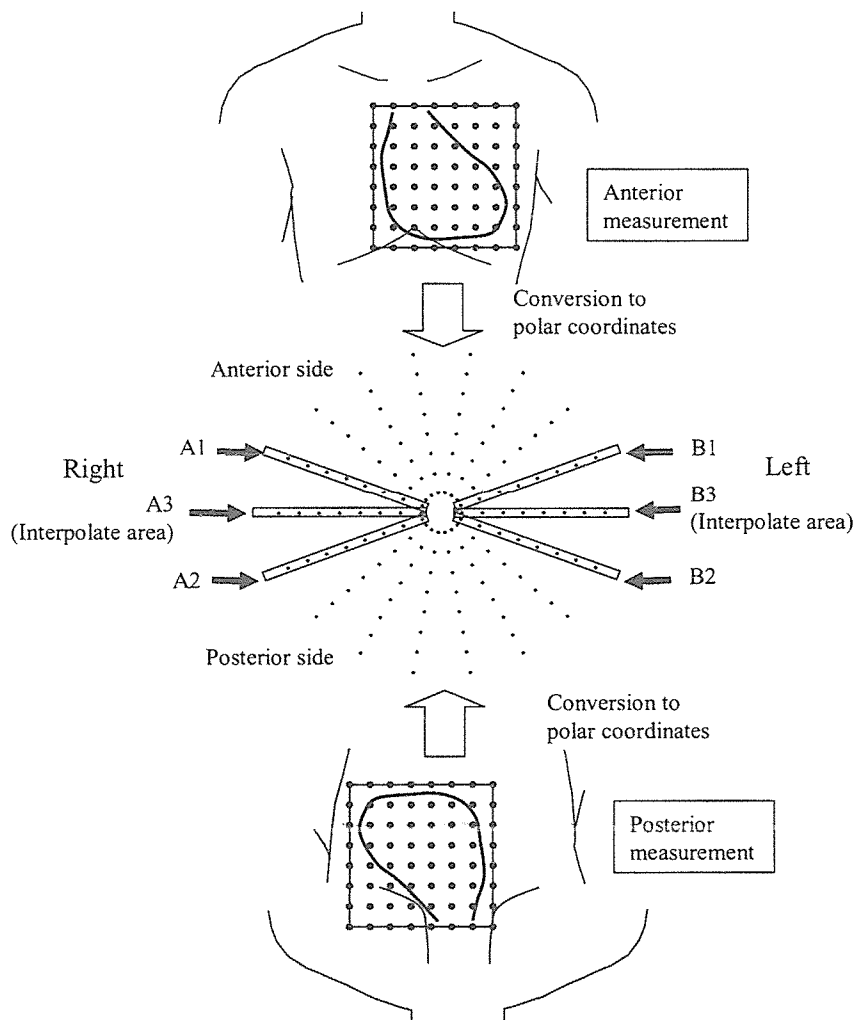
Figure 1. *Method for calculating WHEBEMs. Two current arrows, which are derived from anterior and posterior MCG data, are converted to polar coordinates. Anterior and posterior coordinates are combined using interpolation area.*

We should note that left and right in this article refer to the designations in the figures.
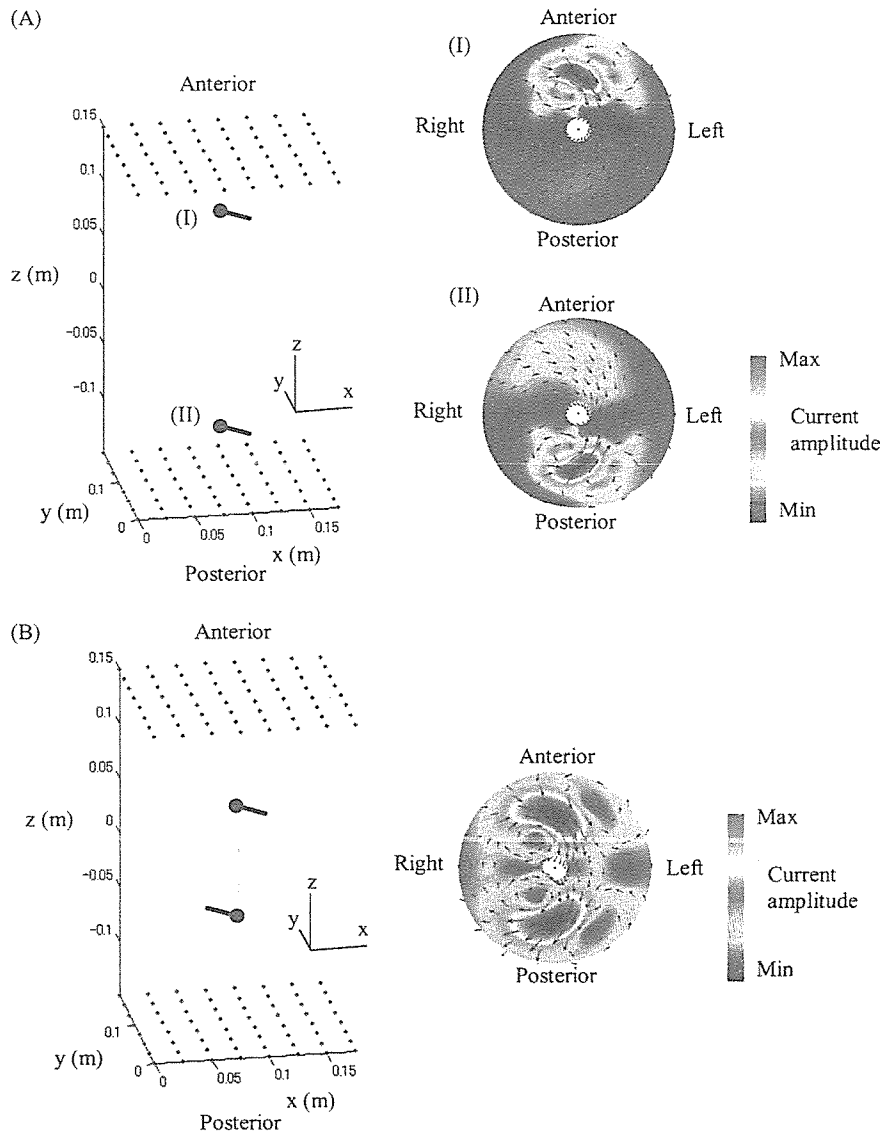
Simulation of WHEBEM

We simulated the WHEBEM using a one-dipole model or two-dipole model to check the map. Simulated WHEBEMs are shown in Figure 2. The one-dipole model has depths from the anterior plane that are (I) 50 and (II) 250 mm, as indicated in Figure 2(A). Its orientation is 45° with respect to the electrical axis of the ECG. The WHEBEM reflects the dipole pattern, depending on the current source. The WHEBEM produced from two dipoles, which are at depths of 100 and 200 mm, is shown in Figure 2(B). The WHEBEM due to two current sources indicates two activations, with one on each side.

In the simulation, we visually estimate the current activation using the WHEBEM. The WHEBEM is used to understand activated sites throughout the heart.

WHEBEM Aanalysis

We analyze abnormal current propagation in Brugada syndrome and CRBBB patients during depolarization. The WHEBEMs correspond to when the R-wave peak and S-wave peak are made. In the maps, a maximum-current arrow and a current arrow with more than half the magnitude of the maximum-current arrow are extracted, and these arrows are redrawn in a new WHEBEM. The current activation pattern in depolarization is investigated by using the plotted current arrows.

Figure 2. *Simulation of WHEBEM. (A) One-dipole model. (B) Two-dipole model. Color indicates magnitude of CAM. Magnitude is normalized to maximum-current arrow. All dipoles are set in center of measurement plane.*

Results

WHEBEM Patterns of Controls

Typical WHEBEM patterns of the R-wave and S-wave peaks in one of the normal controls are shown in Figure 3. In the anterior side MCG waveforms of Figure 3(B), the Q-, R-, and S-waves are separate. Two WHEBEMs are produced, one for each of the separated R- and S-wave peaks, as shown in Figure 3(A).

In the WHEBEM of the R-peak, the currents with maximum magnitude appear in the middle of the left anterior side. The current direction is toward the lower left side. On the other hand, the

S-wave current in the WHEBEM has a small magnitude, and the current with the highest magnitude appears mainly in the mid-anterior side. In the figure, another current also appears on the posterior side. The currents flow in the circumferential direction.

### WHEBEM Patterns of Brugada Syndrome Patients

A typical WHEBEM pattern of the R- and S-waves in Brugada syndrome patients is shown in Figure 4. Although the WHEBEM pattern for the R-wave peak is similar to that of the control,
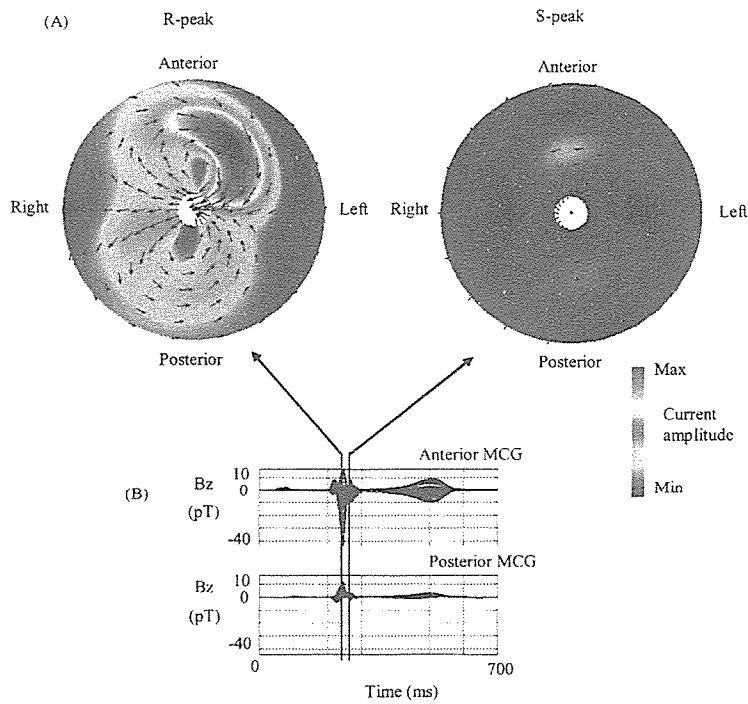
Figure 3. *WHEBEM color maps in case of normal control. (A) R-peak and S-peak WHEBEM color maps; (B) 64 averaged MCG waveforms. Color indicates magnitude of CAM; its magnitude is normalized to maximum-current arrow.*
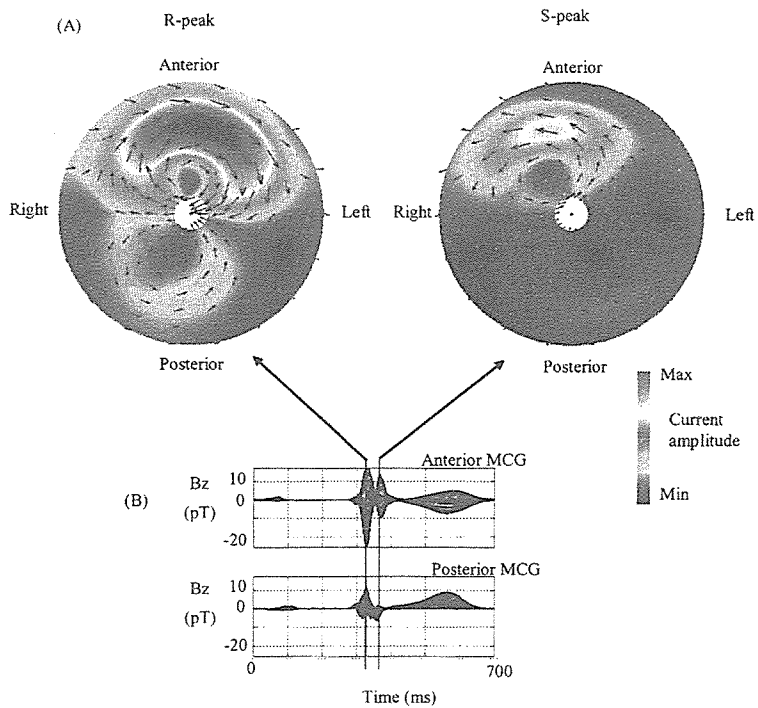
Figure 4. *WHEBEM color maps in the case of Brugada syndrome patients. (A) R-peak and S-peak WHEBEM color maps; (B) 64 averaged MCG waveforms. Color indicates magnitude of CAM; its magnitude is normalized to maximum-current arrow.*
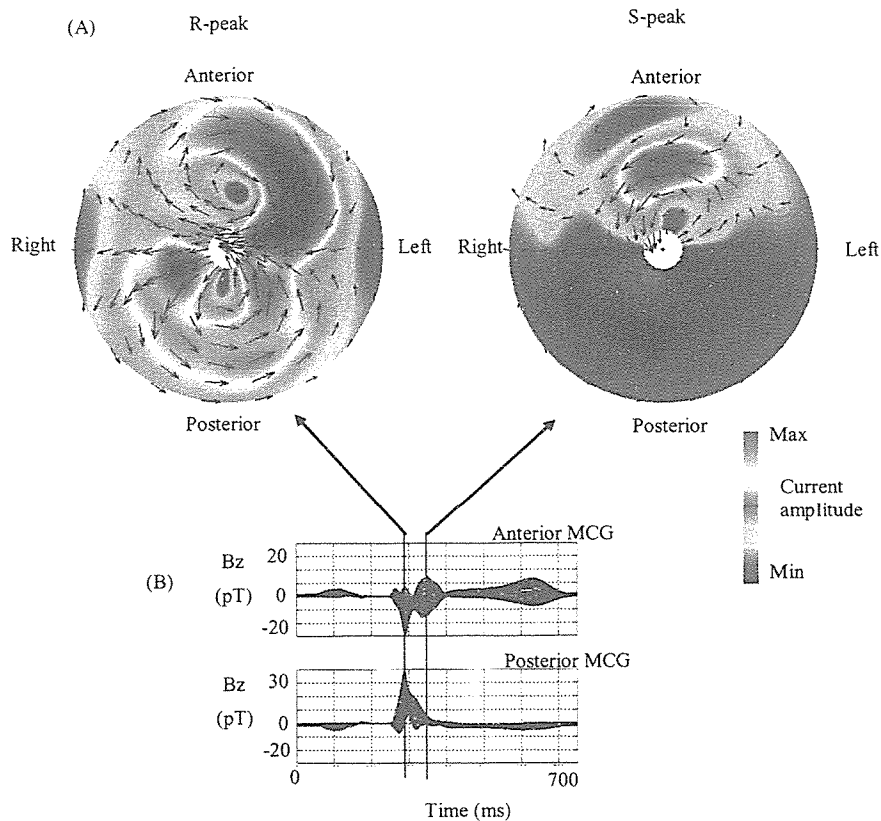
Figure 5. *WHEBEM color maps in the case of CRBBB patients. (A) R-peak and S-peak WHEBEM color maps; (B) 64 averaged MCG waveforms. Color indicates magnitude of CAM; its magnitude is normalized to maximum-current arrow.*

R-vectors in the circumferential direction occur over a large area on the mid-anterior side. The S-current in the upper-right radial direction is larger than that in the control of Figure 3. In the case of the patients, the abnormal S-vector only appears on the anterior side, and four patients had a current with a small magnitude in the mid-posterior side (see Fig. 6). Similar typical patterns exhibited by patients with an S-wave current that has a small magnitude can be seen in 75% (12/16) of the patients, which was not correlated to whether those patients had symptomatic or asymptomatic Brugada syndrome. On the other hand, one of the two Brugada syndrome patients with CRBBB exhibits a typical pattern. However, the difference due to CRBBB remains unclear because we only have data of two patients with Brugada syndrome and CRBBB.

### WHEBEM Patterns of CRBBB Patients

A typical WHEBEM pattern of the S-wave in the case of CRBBB patients is shown in Figure 5(A). In the anterior and posterior MCG waveforms of Figure 5(B), the QRS-complex width is larger

than that of the controls and Brugada syndrome patients. The anterior waveforms have two or three peaks, which characterize the right-branch-block pattern.

In the WHEBEM pattern of the R-wave, the current distribution has two large circular patterns on both the anterior and posterior sides. The abnormal R-wave pattern is shown in 7 out of 10 patients, as shown in Figure 6. On the other hand, the main currents of the S-wave have a large peak in a small mid-anterior area of the hearts of Brugada or control patients. The direction of the large dominant current direction is from the left to the right side. A current with a large amplitude in the S-wave occurs in all CRBBB patients, as shown in Figure 6.

Characterization of WHEBEM Patterns in Controls, Brugada Syndrome Patients, and CRBBB Patients

The main currents (including the current with half the amplitude of the maximum current) were detected, and the detected currents are plotted in the WHEBEM shown in Figure 6.
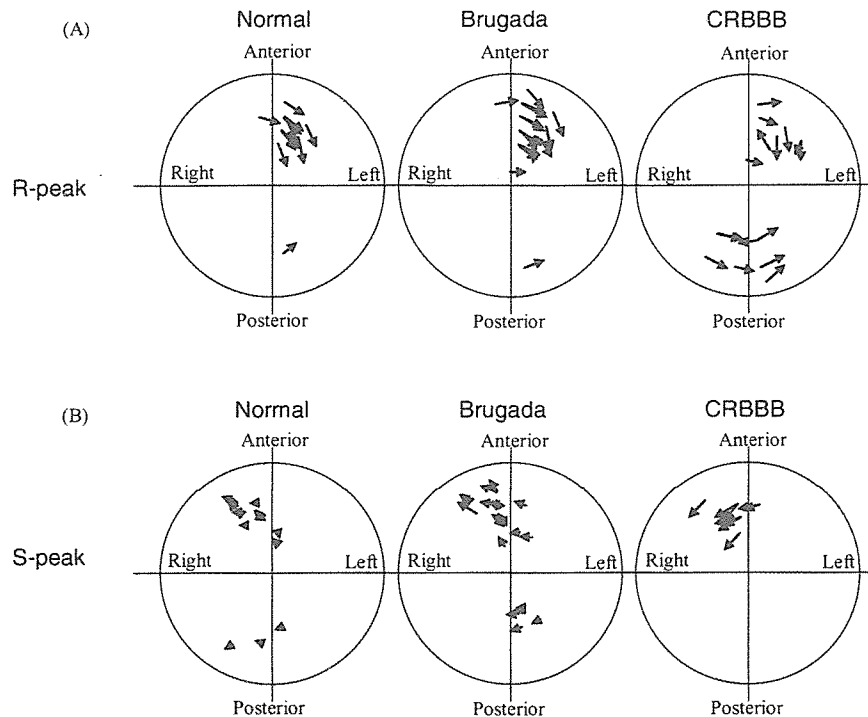
Figure 6. *Main current vector distribution in WHEBEMs at (A) R-peak, and (B) S-peak.*

In Figure 6(A), although the differences between the R- and S-waves of the controls and Brugada syndrome patients are small, small differences can be seen in the S-wave-vector direction and in R-waves scattered over a large area. On the other hand, the CRBBB patients exhibit patterns of the R-wave split between the anterior and posterior sides. Furthermore, the S-wave currents occur in a small area of the anterior side with a similar direction.

The differences and similarities in the dominant currents among control, Brugada syndrome and CRBBB patients are shown in Figure 7, where green arrows indicate the R-wave current and pink arrows indicate the S-wave current. The circles in the figure indicate the distribution of those currents.

In Figure 7, Brugada syndrome patients exhibit a characteristic S-wave pattern, and the R-wave currents are distributed in the area indicated by the circle. CRBBB patients exhibit a large R-wave peak on the anterior and posterior sides, and an S-wave current with the same amplitude as that of the R-wave current appears pointing in the direction from the left to right ventricle.

Discussion

A WHEBEM can visualize the electrical-current distribution that occurs over the area of the epicardial activation throughout the heart. By using a WHEBEM, we focus on simplifying the visual of the main activation during depolarization, in particular, the R- and S-waves. Therefore, we can understand the electrical activation in the left anteromedian, the anteroseptum, and the left posteromedian regions. The WHEBEMs identified activated locations and the difference in direction between abnormal currents in those who have Brugada syndrome and those who have CRBBB, as shown in Figure 6.

In Figure 7, summarized results of S-wave abnormalities in the anteroseptum region of Brugada syndrome patients and CRBBB patients are shown. The abnormality has a different current direction and strength in each case. The abnormal appearance of current vectors may cause a conduction delay in the right ventricle, which was studied by body-surface mapping[10] and Doppler echocardiography.[18] That is because the abnormal current of the S-wave of Brugada syndrome patients activates the right ventricle shortly after the main ventricle activation. The abnormal occurrence of right ventricle activation may result in the lack of activation of the posterosuperior septum area at the time of the R-wave.[17]

Our results regarding patients with Brugada syndrome indicated that the R- and S-wave activation positions on the anterior side are distributed. If the distribution is associated with the abnormal current appearance in the RVOT area at the time

Anterior   Posterior
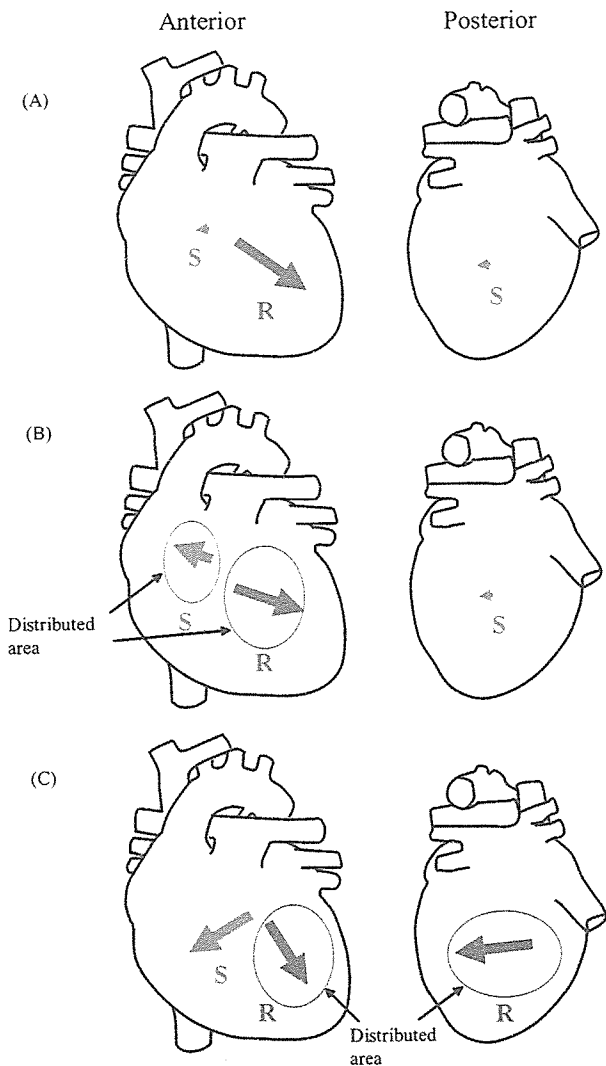
Figure 7. *Summarized main current vectors in (A) controls, (B) Brugada syndrome, and (C) CRBBB are superimposed on heart shape. Blue arrows indicate R-vector, and pink arrows indicate S-vector. Circles indicate distributed area of current vectors.*

of the ST segment,[17] that may be an unexpected indicator of epicardial reentry or VF (or premature ventricular contraction[PVC]) initiation, which is induced at the free-wall region of the RVOT area.[11] Furthermore, the distribution may suggest the existence of an epicardial current dispersion because

the MCG visualizes the epicardial current distribution with a high resolution.[9] If the current distribution is related to the instability of depolarization, the distribution in the Brugada syndrome patient group and daily fluctuations in such individuals may indicate the risk of fatal ventricular arrhythmias in patients with Brugada syndrome.[19] If we obtain MCG data of Brugada syndrome patients daily, the instability of the abnormal current vectors of each patient would be detectable. That instability is an indicator of a high-risk condition.

In the case of CRBBB patients, the large S-vector, which indicates a delay conduction (about 65 ms),[17] only occurs in the anteroseptum area. The visualized S-vector indicates that electrical activation in the ventricles propagates from left to right. The R-vectors of CRBBB patients are distributed in both the anterior and posterior sides. The distribution may indicate the presence of an unstable electrical conduction in the left Purkinje fibers.

We used WHEBEMs to investigate the difference in the ventricular depolarization of the whole heart in the case of Brugada syndrome and CRBBB patients. Consequently, we conclude that Brugada syndrome patients have abnormally distributed R- and S-wave currents, and the abnormalities can be visualized by using WHEBEM. To obtain more information concerning these diseases, combining WHEBEMs and WHEADs (whole-heart electrical-activation diagrams)[17] may be useful.

Study limitations

There are several limitations to this study. First, although the WHEBEM is a powerful tool for understanding the spatial distribution of a ventricular activation current, our findings may differ from findings based on direct measurement of the transmembrane potential because a WHEBEM is a topographic image. Second, we need to study many patients or perform a multicenter investigation to define the diagnostic criteria. Although our results are preliminary because of the above limitations, they are important in terms of understanding the mechanism and clinical implications of Brugada syndrome.

References

1. Brugada P, Brugada J. Right bundle branch block, persistent ST-segment elevation, and sudden cardiac death: A distinct clinical and electrocardiographic syndrome. A multicenter report. J Am Coll Cardiol 1992: 20:1391–1396.
2. Brugada P, Brugada R, Brugada J. Sudden death in patients and relatives with the syndrome of right bundle branch block, ST segment elevation in the precordial leads V(1) to V(3), and sudden death. Eur Heart J 2000: 21:321–326.
3. Brugada R, Brugada J, Antzelevitch C, et al. Sodium channel blockers identify risk for sudden death in patients with ST-segment elevation and right bundle branch block but structurally normal hearts. Circulation 2000: 101:510–515.

4. Ikeda T. Brugada syndrome: Current clinical aspects and risk stratification. Ann Electrocardiol. 2002: 7:251–262.
5. Priori SG, Napolitano C, Gasparini M, et al. Clinical and genetic heterogeneity of right bundle branch block and ST-segment elevation syndrome: A prospective evaluation of 52 families. Circulation 2000: 102:2509–2515.
6. Shimizu W, Antzelevitch C, Suyama K, et al. Effect of sodium channel blockers on ST segment, QRS duration, and corrected QT interval in patients with Brugada syndrome. J Cardiovasc Electrophysiol 2000: 11:1320–1329.
7. Shimizu W, Matsuo K, Takagi M, et al. Body surface distribution and response to drugs of ST segment elevation in Brugada syndrome: Clinical implication of eighty-seven-lead body surface potential mapping and its application to twelve-lead electrocardiograms. J Cardiovasc Electrophysiol 2000: 11:396–404.
8. Yan GX, Antzelevitch C. Cellular basis for the Brugada syndrome and other mechanisms of arrhythmogenesis associated with ST segment elevation. Circulation 1999: 100:1660–1666.
9. Kandori A, Shimizu W, Yokokawa M, et al. Detection of spatial repolarization abnormalities in patients with LQT1 and LQT2 forms of congenital long-QT syndrome. Physiol Meas 2002: 23:603–614.
10. Antzelevitch C, Brugada P, Borggrefe M, Brugada J, Brugada R, Corrado D, Gussak I, et al. Brugada syndrome: Report of the second consensus conference. Heart Rhythm 2005: 2:429–440.
11. Morita H, Fukushima-Kusano K, Nagase S, et al. Site-specific arrhythmogenesis in patients with Brugada syndrome. J Cardiovasc Electrophysiol 2003: 14:373–379.
12. Hosaka H, Cohen D. Visual determination of generators of the magnetocardiogram. J Electrocardiol 1976; 9:426–432.
13. Tsukada K, Kandori A, Miyashita T, Sasabuti H, Suzuki H, Kondo S, Komiyama Y, et al. A simplified superconducting interference device system to analyze vector components of a cardiac magnetic field. Proceedings 20th International Conference IEEE/EMBS (Hong Kong) 1998; 524–527.
14. Yamada S, Yamaguchi I. Magnetocardiograms in clinical medicine: Unique information on cardiac ischemia, arrhythmias, and fetal diagnosis. Intern Med 2005: 44:1–419.
15. Fenici R, Brisinda D, Meloni AM. Clinical application of magnetocardiography. Expert Rev Mol Diagn. 2005; 5(3):291–313.
16. Kandori A, Shimizu W, Yokokawa M, et al. Identifying patterns of spatial current dispersion that characterize and separate the Brugada syndrome and complete right-bundle branch block. Med Biol Eng Comput 2004: 42:236–244.
17. Kandori A, Miyashita T, Ogata K, Shimizu W, Yokokawa M, Kamakura S, Miyatake K, et al. Electrical space-time abnormalities of ventricular depolarization in patients with Brugada syndrome and patients with complete right-bundle branch blocks studied by magnetocardiography. Pacing Clin Electrophysiol 2006; 29(1):15–20.
18. Tukkie R, Sogard P, Vleugels J, et al. Delay in right ventricular activation contributes to Brugada syndrome. Circulation 2004: 109:1272–1277.
19. Tatsumi H, Takagi M, Nakagawa E, Yamashita H and Yoshiyama M,. Risk stratification in patients with Brugada syndrome: Analysis of daily fluctuations in 12-lead electrocardiogram (ECG) and signal-averaged electrocardiogram (SAECG). J Cardiovasc Electrophysiol. 2006; 17(7):705–711.

Sex Hormone and Gender Difference—Role of Testosterone on Male Predominance in Brugada Syndrome

WATARU SHIMIZU, M.D., PH.D.,* KIYOTAKA MATSUO, M.D., PH.D.,†
YOSHIHIRO KOKUBO, M.D., PH.D.,‡ KAZUHIRO SATOMI, M.D., PH.D.,*
TAKASHI KURITA, M.D., PH.D.,* TAKASHI NODA, M.D., PH.D.,*
NORITOSHI NAGAYA, M.D., PH.D.,* KAZUHIRO SUYAMA, M.D., PH.D.,*
NAOHIKO AIHARA, M.D.,* SHIRO KAMAKURA, M.D., PH.D.,*
NOZOMU INAMOTO, M.D., PH.D.,‡ MASAZUMI AKAHOSHI, M.D., PH.D.,¶
and HITONOBU TOMOIKE, M.D., PH.D.*

From the *Division of Cardiology, Department of Internal Medicine; ‡Department of Preventive Cardiology, National Cardiovascular Center, Suita, Japan; †Department of Cardiovascular Medicine, Nagasaki University Graduate School of Medicine; and ¶Department of Clinical Studies, Radiation Effects Research Foundation, Nagasaki, Japan

Testosterone in Brugada Syndrome. *Introduction:* The clinical phenotype is 8 to 10 times more prevalent in males than in females in patients with Brugada syndrome. Brugada syndrome has been reported to be thinner than asymptomatic normal controls. We tested the hypothesis that higher testosterone level associated with lower visceral fat may relate to Brugada phenotype and male predominance.

Methods and Results: We measured body-mass index (BMI), body fat percentage (BF%), and several hormonal levels, including testosterone, in 48 Brugada males and compared with those in 96 age-matched control males. Brugada males had significantly higher testosterone (631 ± 176 vs 537 ± 158 ng/dL; P = 0.002), serum sodium, potassium, and chloride levels than those in control males by univariate analysis, and even after adjusting for age, exercise, stress, smoking, and medication of hypertension, diabetes, and hyperlipidemia, whereas there were no significant differences in other sex and thyroid hormonal levels. Brugada males had significantly lower BMI (22.1 ± 2.9 vs 24.6 ± 2.6 kg/m^2; P < 0.001) and BF% (19.6 ± 4.9 vs 23.1 ± 4.7%; P < 0.001) than control males. Testosterone level was inversely correlated with BMI and BF% in both groups, even after adjusting for the confounding variables. Conditional logistic regression models analysis showed significant positive and inverse association between Brugada syndrome and hypertestosteronemia (OR:3.11, 95%CI:1.22–7.93, P = 0.017) and BMI (OR:0.72, 95%CI:0.61–0.85, P < 0.001), respectively.

Conclusions: Higher testosterone level associated with lower visceral fat may have a significant role in the Brugada phenotype and male predominance in Brugada syndrome. *(J Cardiovasc Electrophysiol, Vol. 18, pp. 415-421, April 2007)*

Brugada syndrome, gender, sex hormones, testosterone, body mass index

Introduction

Brugada syndrome is characterized by coved-type ST-segment elevation in the right precordial electrocardiographic (ECG) leads (V1–V3) and an episode of ventricular fibrillation (VF) in the absence of structural heart disease.[1-5] The

prevalence of the disease is estimated to be up to 5 per 10,000 inhabitants and is one of the important causes of sudden cardiac death of middle-aged males, particularly in Asian countries including Japan.[4]

More than eight dozen distinct mutations in *SCN5A*, the gene encoding the α subunit of the sodium channel, have been so far identified in patients with Brugada syndrome and all mutations display an autosomal-dominant mode of transmission.[6,7] Therefore, males and females are expected to inherit the defective gene equally. However, more than 80% of patients in Western countries and more than 90% of patients in Asian countries affected with Brugada syndrome are males.[8] Recent experimental studies have unveiled the cellular mechanism of Brugada phenotype. The male predominance in the Brugada syndrome is suggested to be due, at least in part, to intrinsic differences in ventricular action potential (AP) between males and females.[9]

A male hormone, testosterone is reported to increase net outward currents[10-12] and is expected to accentuate Brugada phenotype, such as ST-segment elevation and subsequent episodes of VF in patients with Brugada syndrome. Testosterone is also known to decrease visceral fat.[13-15] Since patients with Brugada syndrome have been reported to be

thinner than asymptomatic normal controls by Matsuo et al.,[16] we speculated that higher testosterone level associated with lower visceral fat may modulate Brugada phenotype and may relate to male predominance in patients with Brugada syndrome.

Methods

Patient Population and Data Collection

The study population consisted of 48 males with Brugada syndrome who agreed to participate in this study and showed Type 1 "coved" ST-segment elevation in V1–V3 leads[17] ranging in age from 30 to 69 years with a mean age of 50 ± 11 years (mean $\pm$ SD). Brugada males who were less than 30 years old and more than 70 years old were excluded from this study to minimize the influence of age on the basal sex hormonal levels including testosterone. Forty of the forty-eight Brugada males have been included in our previous clinical studies.[18-20] In all patients, physical examination, chest roentgenogram, laboratory values, echocardiography with wall motion analysis, and Doppler screening excluded structural heart diseases. The clinical, electrocardiographic, and electrophysiologic characteristics of the 48 Brugada males are shown in Table 1. Average age of the 48 Brugada males at diagnosis was 47 ± 12 years old. Aborted cardiac arrest or VF was documented in 21 males (44%), syncope alone in 11 males (23%), and 16 males (33%) were asymptomatic. Family history of sudden cardiac death (SCD) was observed in eight males (17%). An *SCN5A* coding region mutation was identified in seven (17%) of 42 males in whom genetic screening was conducted. Implantable cardioverter defibrillator (ICD) was implanted in all 32 symptomatic males with documented VF and/or syncope. ICD was also implanted in nine of 16 asymptomatic males due to induction of VF during the electrophysiologic study. Type 1 ST-segment elevation was recorded spontaneously in

43 males (90%) and was induced by sodium channel blockers in five males (10%). Complete right bundle branch block was observed in three males (6%). Late potential was recorded by a signal-average ECG system in 27 (59%) of 46 males. During the electrophysiologic study, VF requiring direct cardioversion for termination was induced in 32 (73%) of 44 males. Average HV interval was 46 ± 11 msec.

We first obtained data, such as the hormonal levels, visceral fat parameters, and ECG parameters in the 48 Brugada males prospectively between January and July in 2003, mainly at regular outpatient clinics for checking ICD. Only a Brugada male refused to participate during the recruitment of the case.

Thereafter, age-matched control males were randomly selected from the municipal population registry in Suita City. The hormonal and visceral fat data were collected sequentially between August and December in 2003. The municipal population registry in Suita City included 5,846 control subjects, among whom 1,052 males were age-matched to the 48 Brugada males. The 96 control males with a mean age of 50 ± 11 years were sequentially recruited from the age-matched 1,052 males. None of the recruited 96 control males refused to participate in this study. There were no significant differences in the clinical characteristics between the 96 control males and the remaining 956 age-matched males. Therefore, we had no way of knowing the body weight of the individuals who were selected to serve as controls from a very large database. Although K. Matsuo is a co-author of this study, none of the Brugada males and control males who appeared in the article by Matsuo[16] are included in the present study population.

All protocols were approved by the Ethical Review Committee in the National Cardiovascular Center. Written informed consent was obtained from all subjects.

Sex and Thyroid Hormonal Levels and Serum Electrolytes

Blood samples for analysis of basal hormone levels and serum electrolytes were obtained between 8:00 and 9:00 AM after an overnight fast. Plasma sex hormonal levels including testosterone, estradiol, DHEA-S, LH, and FSH were measured using commercially prepared immunoassay kits (testosterone, LH, and FSH: Chemiluminescent immunoassay [Bayer HealthCare, New York, NY, USA]; estradiol: Electrochemiluminescent immunoassay [Roche Diagnostics GmbH, Mannheim, Germany]; DHEA-S: Radioimmunoassay [Diagnostic Products Corporation, Los Angeles, CA, USA]). Thyroid hormonal levels including free T3, T4, and TSH, and serum electrolyte levels including sodium, potassium, and chloride were also measured.

Body Mass Index and Body Fat Percentage

Body weight (BW) was measured to the nearest 0.1 kg and height to the nearest cm. Body-mass index (BMI) was calculated as weight/height^2 (kg/m^2) as a parameter of visceral fat. We also measured body-fat percentage (BF%) by using body composition analyzer (Biospace Co., Ltd. Tokyo, Japan). These visceral fat parameters were measured just after blood sampling. In the 32 symptomatic Brugada males who had had documented VF and/or syncope, the BW and BMI were also measured within 48 hours after their clinical events during admission in our hospital or other emergent hospitals.

TABLE 1

Clinical, Electrocardiographic, and Electrophysiologic Characteristics in the 48 Brugada Males

Clinical characteristics	
Age at diagnosis (years)	47 ± 12
Aborted cardiac arrest or VF (%)	21/48 (44%)
Syncope alone (%)	11/48 (23%)
Asymptomatic (%)	16/48 (33%)
Family history of SCD	8/48 (17%)
SCN5A mutation	7/42 (17%)
ICD implantation	41/48 (85%)
Follow-up period (month)	41 ± 2
Arrhythmic event (%)	9/48 (19%)
Electrocardiographic characteristics	
Spontaneous coved-type ST elevation	43/48 (90%)
CRBBB (%)	3/48 (6%)
RR (msec)	939 ± 113
PQ interval (II) (msec)	186 ± 34
QRS duration (V2) (msec)	104 ± 18
Corrected QT interval (V5) (msec)	394 ± 27
ST amplitude at J point (V2) (mV)	0.32 ± 0.16
Late potential (%)	27/46 (59%)
Electrophysiologic characteristics	
Induction of VF	32/44 (73%)
Mode (Triple/Double/Single)	16/15/1
HV interval (msec)	46 ± 11

CRBBB = complete right bundle branch block; ICD = implantable cardioverter defibrillator; SCD = sudden cardiac death; VF = ventricular fibrillation.

ECG Parameters

In the 48 males with Brugada syndrome, 12-lead ECG was recorded just before blood sampling, and ECG parameters were assessed by an investigator (WS) blinded to clinical information. The ECG parameters included RR interval, PQ interval measured in lead II, QRS interval measured in lead V2, QT interval, corrected QT (QTc) interval measured in leads V5, and ST amplitude at J point measured in lead V2.

Statistical Analysis

We first conducted univariate analysis by using unpaired *t*-test to compare each data between the Brugada males and the control males. Since several confounding variables, such as age, exercise (none, sometimes, regularly), stress (none, sometimes, regularly), current smoking (no, yes), and medication (no, yes) of hypertension, diabetes, and hyperlipidemia may affect the hormonal levels including testosterone level and the visceral fat parameters, analysis of covariance (ANCOVA) was used to compare least square mean values between the Brugada males and the control males adjusting for these confounding variables. Pearson's correlation coefficients were calculated between the testosterone level and the visceral fat parameters. Partial correlation coefficients were calculated between the testosterone level and the visceral fat parameters after adjusting for age, exercise, stress, current smoking, and medication. Moreover, conditional logistic regression models were used to calculate odds ratios and 95% confidence intervals adjusting for age, BMI, exercise, stress, current smoking, hypertension, diabetes, and hyperlipidemia. Hypertestosteronemia was defined as serum testosterone levels ≥700 ng/dL, which is 75 percentiles of testosterone levels among case and control combined groups. In the 32 Brugada males with documented VF and/or syncope, a paired *t*-test was used to compare the visceral fat parameters at the clini-

cal cardiac events and at the measurement of hormonal and visceral fat data. A two-sided P value below 0.05 was considered to indicate significance. All statistical analyses were performed by using SAS software, Ver 8.2.

Results

Hormonal Levels, Serum Electrolytes, and Visceral Fat

Table 2 illustrates univariate analysis for comparing sex and thyroid hormonal levels, serum electrolytes, and visceral fat parameters between the two groups. Testosterone level was significantly higher in the Brugada males than in the control males, whereas there were no significant differences in other sex hormonal levels; estradiol, DHEA-S, LH, FSH, and thyroid hormonal levels; T3, T4, and TSH. Serum sodium, potassium, and chloride levels were all significantly higher in the Brugada males than in the control males. BMI, BF%, and BW were all significantly lower in the Brugada males than in the control males. All variables followed normal distribution, both in the 48 Brugada and 96 control males.

The comparison of the confounding variables that may affect the hormonal levels and the visceral fat parameters between the 48 Brugada males and the 96 control males was shown in Table 3. Even after adjusting for age, exercise, stress, current smoking, and medication (hypertension, diabetes, and hyperlipidemia), the testosterone level, serum sodium, potassium, and chloride levels were all significantly higher, and the visceral fat parameters were significantly lower in the 48 Brugada males than in the 96 control males (Table 4). There were also significant differences in these parameters between the 24 definite Brugada males with documented VF and/or *SCN5A* mutations and the 96 control males after adjusting for the confounding variables (Table 4).

Correlation between Testosterone, Visceral Fat, and Serum Electrolytes

Testosterone level was inversely correlated with all visceral fat parameters, BMI, BF%, or BW in both the Brugada males and the control males, even after adjusting for age,

TABLE 2

Sex and Thyroid Hormonal Levels, Serum Electrolytes, and Visceral Fat Parameters in the 48 Brugada Males and the 96 Age-Matched Control Males

	Brugada Males (n = 48)	Control Males (n = 96)	P Value
Sex hormones			
Testosterone (ng/dL)	631 ± 176	537 ± 158	0.002
Estradiol (pg/mL)	28.9 ± 7.6	31.1 ± 12.6	0.263
DHEA-S (ng/mL)	1,901 ± 850	1,966 ± 861	0.668
LH (mIU/mL)	4.6 ± 2.6	3.9 ± 2.0	0.073
FSH (mIU/mL)	6.2 ± 4.9	5.0 ± 2.9	0.066
Thyroid hormones			
Free T3 (pg/mL)	3.3 ± 0.4	3.4 ± 0.3	0.360
Free T4 (ng/dL)	1.3 ± 0.1	1.3 ± 0.2	0.089
TSH (μIU/mL)	1.9 ± 1.4	1.7 ± 1.4	0.619
Serum electrolytes			
Sodium (mEq/L)	143.7 ± 2.0	142.6 ± 2.0	0.003
Potassium (mEq/L)	4.6 ± 0.3	4.3 ± 0.3	<0.001
Chloride (mEq/L)	105.1 ± 2.1	103.6 ± 2.1	<0.001
Viceral fat			
BMI (kg/m²)	22.1 ± 2.9	24.6 ± 2.6	<0.001
BF% (%)	19.6 ± 4.9	23.1 ± 4.7	<0.001
BW (kg)	62.9 ± 9.7	70.0 ± 8.6	<0.001

Values are mean ± SD where indicated.
BMI = body-mass index; BF% = body-fat percentage; BW = body weight.

TABLE 3

Comparison of the Confounding Variables Between the 48 Brugada Males and the 96 Age-Matched Control Males

	Brugada Males (n = 48)	Control Males (n = 96)	P Value
Exercise			
None (%)	39.6	44.8	
Sometimes (%)	41.6	43.8	
Regularly (%)	18.8	11.5	0.482
Stress			
None (%)	27.1	21.9	
Sometimes (%)	54.2	54.2	
Regularly (%)	18.8	24.0	0.684
Current smoking (%)	25.0	27.1	0.789
Medication			
Hypertension (%)	20.8	19.8	0.883
Diabetes (%)	2.1	13.5	0.028
Hyperlipidemia (%)	10.4	5.2	0.246

TABLE 4

Testosterone, Serum Electrolytes, and Visceral Fat Parameters in the Brugada Males and the 96 Age-Matched Control Males after Adjusting for Confounding Variables

	Brugada Males	Control Males (n = 96)	P Value
ALL Case (n = 48)			
Testosterone (ng/dL)	631 ± 44	538 ± 40	0.003
Sodium (mEq/L)	144.2 ± 0.5	143.2 ± 0.5	0.007
Potassium (mEq/L)	4.6 ± 0.1	4.3 ± 0.1	<0.001
Chloride (mEq/L)	105.5 ± 0.5	103.9 ± 0.5	<0.001
BMI (kg/m^2)	22.3 ± 0.7	24.9 ± 0.7	<0.001
BF% (%)	20.0 ± 1.3	23.9 ± 1.1	<0.001
BW (kg)	63.4 ± 2.4	70.1 ± 2.1	0.001
Definite Brugada case with VF and/or *SCN5A* (n = 24)			
Testosterone (ng/dL)	656 ± 59	550 ± 48	0.009
Sodium (mEq/L)	143.9 ± 0.7	142.9 ± 0.6	0.042
Potassium (mEq/L)	4.7 ± 0.1	4.4 ± 0.1	<0.001
Chloride (mEq/L)	105.2 ± 0.7	103.9 ± 0.6	0.006
BMI (kg/m^2)	21.5 ± 1.0	24.5 ± 0.8	<0.001
BF% (%)	19.9 ± 1.7	24.1 ± 1.4	<0.001
BW (kg)	60.5 ± 3.1	69.2 ± 2.5	0.001

Values are mean ± SE adjusted for age, exercise, stress, current smoking, and medication of hypertension, diabetes and hyperlipidemia. BMI = body-mass index; BF% = body-fat percentage; BW = body weight; VF = ventricular fibrillation.

exercise, stress, current smoking, and medication (Brugada: BMI, $r = -0.394$, $P = 0.011$; BF%, $r = -0.390$, $P = 0.012$; BW, $r = -0.335$, $P = 0.032$; Control: BMI, $r = -0.333$, $p = 0.002$; BF%, $r = -0.333$, $P = 0.001$; BW, $r = -0.305$, $P = 0.004$), suggesting that Brugada males had higher testosterone level associated with lower visceral fat compared with control males (Fig. 1). No significant correlations were observed between other serum electrolytes and testosterone level or visceral fat parameters. Testosterone level was not correlated with age, even after adjusting for exercise, stress, current smoking, and medication ($r = 0.007$, $P = 0.947$).

Conditional Logistic Regression Models Analysis

Conditional logistic regression models analysis showed significant positive and inverse association between Brugada syndrome, hypertestosteronemia (Odd Ratio (OR): 3.11, 95%CI: 1.22–7.93, P = 0.017), and BMI (OR: 0.72, 95%CI: 0.61–0.85, P < 0.001), respectively (Table 5). Other variables did not significantly increase or decrease risks of Brugada syndrome (Table 5).

Visceral Fat at Clinical Cardiac Events in Brugada Males

In the 32 symptomatic Brugada males with documented VF and/or syncope, the time-span between the clinical cardiac events and the measurement of hormonal and the visceral fat data was 42 ± 32 months (mean ± SD, 1–99 months). The BMI and BW at the clinical cardiac events (VF or syncope) were significantly lower than those at the measurement of hormonal and visceral fat data (BMI, 21.0 ± 2.6 vs 22.1 ± 2.9 kg/m^2; BW, 60.0 ± 8.9 vs 62.9 ± 9.7 kg: P < 0.001, respectively).

Testosterone versus ECG Parameters, Symptoms or SCN5A Mutation in Brugada Males

Baseline electrocardiographic data of the 48 Brugada males are shown in Table 1. No significant correlations were observed between testosterone level and ECG parameters, including ST amplitude ($r = -0.123$, $P = 0.406$) and QTc interval ($r = -0206$, $P = 0.160$), in the 48 Brugada males. There was no significant difference in testosterone level between 32 symptomatic and 16 asymptomatic Brugada males (649 ± 185 vs 593 ± 157 ng/dL: P = 0.298). No significant difference was observed in testosterone level between 43 Brugada males with spontaneous Type 1 ST-segment elevation and five Brugada males with sodium channel blocker-induced Type 1 ST-segment elevation (624 ± 171 vs 688 ± 230 ng/dL: P = 0.448). Testosterone level was also no different between seven Brugada males with *SCN5A* mutation and 41 Brugada males without *SCN5A* mutation (700 ± 198 vs 619 ± 172 ng/dL: P = 0.261).

Follow-Up

Arrhythmic events occurred in nine (19%) of 48 Brugada males during average follow-up periods of 41 ± 2 months after blood sampling for the present study (Table 1). In more detail, arrhythmic events appeared in eight (38%) of 21 Brugada males with a history of aborted cardiac arrest or VF, in one (9%) of 11 Brugada males with syncope alone, but did not appear in any (0%) of 16 asymptomatic Brugada males.

Discussion

The major findings of the present study were: (1) Brugada males had significantly higher testosterone level, serum sodium, potassium, and chloride level, and significantly lower BMI, BF%, and BW than those in control males by univariate analysis, even after adjusting for age, exercise, stress, current smoking, and medications related to hypertension, diabetes and hyperlipidemia. (2) Testosterone level was inversely correlated with the BMI, BF%, and BW in both Brugada males and control males, even after adjusting for the confounding variables. (3) Conditional logistic regression models analysis showed strong positive association between Brugada syndrome and higher testosterone level (hypertestosteronemia) and strong inverse association between Brugada syndrome and BMI.

Testosterone in Brugada Phenotype and Male Predominance

For the past decade, numerous clinical, experimental, and molecular genetic studies have elucidated Brugada syndrome as a distinct clinical entity.[1-5,17] However, several problems remain unresolved, such as genetic heterogeneity, ethnic difference, and gender difference.[7] Di Diego and Antzelevitch recently suggested the cellular basis for male predominance in Brugada syndrome by using arterially perfused canine right ventricular wedge preparations.[9] Transient outward current (I_{to})-mediated phase 1 AP notch was larger in male dogs than in female dogs in the right ventricular epicardium, but not in the left ventricular epicardium, responsible for the male predominance in the Brugada phenotype. Recent clinical studies suggested that male hormone testosterone might be attributable to gender difference of the prevalence in this
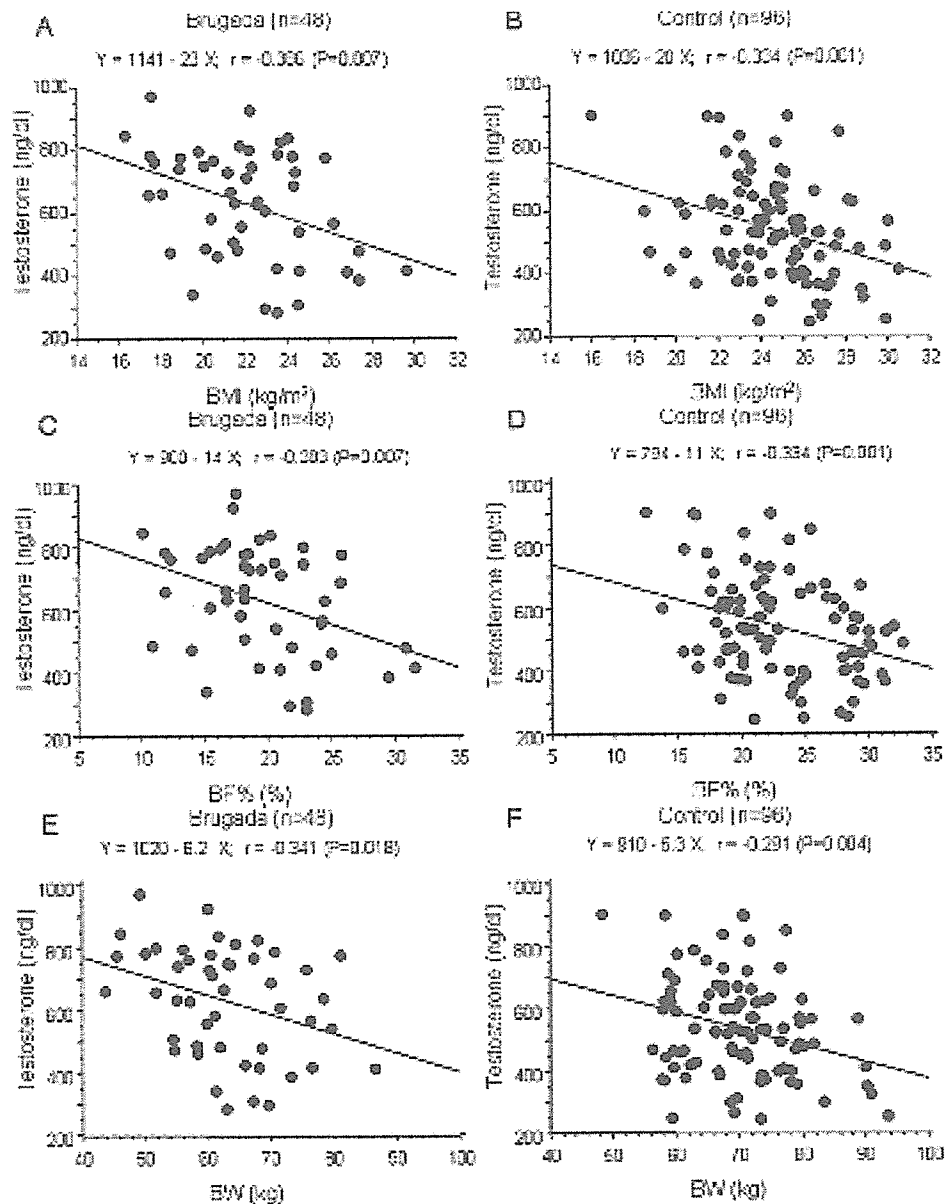
Figure 1. *Correlation between testosterone level and visceral fat parameters: body mass index (BMI) (A and B), body fat percentage (BF%) (C and D), and body weight (BW) (E and F) in the 48 Brugada males and the 96 age-matched control males. Testosterone level was inversely correlated with the BMI, BF%, or BW in both Brugada males and control males.*

syndrome. Matsuo et al. reported two cases of asymptomatic Brugada syndrome in whom typical coved ST-segment elevation disappeared following orchiectomy as therapy for prostate cancer,[21] indicating that testosterone may contribute to the Brugada phenotype in these two cases. Several experimental studies reported that testosterone increased outward potassium currents, such as the rapidly activating component (I_{Kr})[10,11] and the slowly activating component (I_{Ks})[12] of the delayed rectifier potassium current, and the inward rectifier potassium current (I_{K1}),[11] or decreased inward L-type calcium current (I_{Ca-L}).[12] Since the maintenance of the AP dome is determined by the fine balance of currents active at the end of phase 1 of the AP (principally I_{to} and I_{Ca-L}),[22,23] any agents that increase outward currents or decrease inward currents can increase the magnitude of the AP notch, leading

to loss of the AP dome (all-or-none repolarization) in the epicardium, but not in the endocardium, contributing to a significant voltage gradient across the ventricular wall during ventricular activation, thus augmenting ST-segment elevation, the Brugada phenotype.[24] Therefore, testosterone would be expected to accentuate the Brugada phenotype. In the present study, males with Brugada syndrome had significantly higher testosterone level than age-matched control males, even after adjusting for age, exercise, stress, current smoking, and medication (hypertension, diabetes, and hyperlipidemia), which may affect the testosterone level. Moreover, conditional logistic regression models analysis showed strong positive association between Brugada syndrome and higher testosterone level (OR: 3.11). Our data suggest a significant role of testosterone, male hormone, in the Brugada phenotype. The

TABLE 5

Odds Ratios of Presence of Hypertestosteronemia and Confounding Risk Factors for Brugada Syndrome in Males

Variable	Odd Ratio	95% Confidence Interval	P Value
Hypertestosteronemia	3.11	1.22–7.93	0.017
Age	0.99	0.95–1.03	0.637
BMI	0.72	0.61–0.85	<0.001
Exercise	1.57	0.87–2.83	0.135
Stress	0.69	0.35–1.35	0.277
Current smoking	0.71	0.26–1.90	0.493
Hypertension	3.12	0.85–11.45	0.087
Diabetes	0.13	0.01–1.27	0.079
Hyperlipidemia	2.14	0.44–10.49	0.348

Hypertestosteronemia was defined as serum testosterone levels $\geq$ 700 ng/dL.

data also indicate that the male predominance in the Brugada phenotype is at least in part due to testosterone, which is present only in males.

Lower Visceral Fat May Be a Predictor for Brugada Phenotype

Matsuo et al. recently reported in their epidemiologic study that cases with the Brugada-type ECG had significantly lower BMI than that in control subjects.[16] Similarly, in the present study, males with Brugada syndrome had significantly lower visceral fat parameters, BMI, BF%, and BW than those in age-matched control males, even after adjusting for several confounding variables. Moreover, conditional logistic regression models analysis showed strong inverse association between Brugada syndrome and BMI (OR: 0.72). All of the visceral fat parameters were inversely correlated with testosterone level in both Brugada and control males, even after adjusting for the confounding variables. It has been well demonstrated that testosterone level in obese males is decreased compared to normal males of similar age.[13] Tsai et al. reported that lower baseline total testosterone level independently predicted an increase in visceral fat in the Japanese-American male cohort for 7.5 years.[15] Reversely, Marin et al. reported that testosterone treatment of middle-aged abdominally obese males was followed by a decrease of visceral fat mass measured by computerized tomography.[14] These data suggest that primarily higher level of testosterone in Brugada males compared to that in control males may result in lower visceral fat in Brugada males, which would be an "innocent bystander" sign of Brugada phenotype. In reverse, if primary lower visceral fat (body weight loss) would result in higher testosterone level, the weight loss could be a trigger for Brugada phenotype, just like fever is.[25] It is noteworthy that the visceral fat parameters at the clinical cardiac events (VF or syncope) in the 32 symptomatic Brugada males were significantly lower than those at the time of blood sampling for this study. This indicates that testosterone level is expected to be additively higher at the clinical cardiac events, which may contribute to spontaneous episodes of VF or syncope.

Other Hormonal Levels and Serum Electrolytes

Estradiol, female hormone, is reported to reduce the expression of Kv4.3 channels, which are important molecular

components of I_{to} currents.[26] However, in contrast to testosterone, other sex hormonal levels including estradiol were not different between the Brugada males and the control males in the present study. Although thyroid hormones are also demonstrated to alter membrane currents, such as I_{to} and I_{Ca-L},[27,28] no significant differences were observed in the thyroid hormonal levels between the two groups in the present study.

On the other hand, serum sodium, potassium, and chloride levels were all significantly higher in the Brugada males than in the control males, even after adjusting for several confounding variables. Recently, many agents and conditions that cause an outward shift in current activity at the end of phase 1 AP have been known to unmask ST-segment elevation, as found in the Brugada syndrome, leading to the acquired form of this disorder.[4,29] Electrolyte abnormalities, such as hyperkalemia, are reported to amplify ST-segment elevation like that in Brugada syndrome.[30] The lower visceral fat found in the Brugada males is expected to decrease serum level of insulin, leptine, a novel adipocyte-derived hormone, or ghrelin, a novel growth hormone-releasing peptide, suppressing β-adrenergic receptor or plasma norepinephrine level, resulting in an increase of serum potassium level.[31,32] Further studies including measurement of levels of insulin, leptine, and ghrelin will be required to elucidate the precise mechanism.

Study Limitations

Although the testosterone level was significantly higher in the Brugada males than in the control males, no statistically significant correlations were observed between the testosterone level and the ST amplitude in the Brugada males. The degree of the ST-segment elevation is variable between Brugada patients because it is influenced by several factors other than sex hormonal levels or electrolytes levels, such as basal autonomic tone, presence of *SCN5A* mutation, or probably intrinsic current density of I_{to}, etc., in the right ventricular epicardial cells. The threshold of ST-segment elevation for spontaneous induction of VF also varies between Brugada patients. Therefore, the Brugada phenotype, such as ST-segment elevation or spontaneous induction of VF, may correlate with the testosterone level day to day individually (intra-personally) in each Brugada male, but may not correlate among the pooled data obtained from many Brugada males, probably due to inter-person difference of the ST-segment elevation.

There were no significant differences in testosterone level between symptomatic and asymptomatic Brugada males, between Brugada males with spontaneous ST elevation and those with sodium channel blocker-induced ST elevation, or between Brugada males with and without *SCN5A* mutation, all of which are probably due to a relatively small number of Brugada males in the present study. Further evaluation with increasing number of Brugada males will be required.

References

1. Brugada P, Brugada J: Right bundle branch block, persistent ST segment elevation and sudden cardiac death: A distinct clinical and

electrocardiographic syndrome: A multicenter report. J Am Coll Cardiol 1992;20:1391-1396.

2. Brugada J, Brugada R, Brugada P: Determinants of sudden cardiac death in individuals with the electrocardiographic pattern of Brugada syndrome and no previous cardiac arrest. Circulation 2003;108:3092-3096.

3. Priori SG, Napolitano C, Gasparini M, Pappone C, Della Bella P, Giordano U, Bloise R, Giustetto C, De Nardis R, Grillo M, Ronchetti E, Faggiano G, Nastoli J: Natural history of Brugada syndrome: Insights for risk stratification and management. Circulation 2002;105:1342-1347.

4. Antzelevitch C, Brugada P, Borggrefe M, Brugada J, Brugada R, Corrado D, Gussak I, Lemarec H, Nademanee K, Perez Riera AR, Shimizu W, Schulze-Bahr E, Tan H, Wilde A: Brugada syndrome. Report of the second consensus conference. Endorsed by the Heart Rhythm Society and the European Heart Rhythm Association. Circulation 2005;111:659-670.

5. Eckardt L, Probst V, Smits JP, Bahr ES, Wolpert C, Schimpf R, Wichter T, Boisseau P, Heinecke A, Breithardt G, Borggrefe M, Lemarec H, Bocker D, Wilde AA: Long-term prognosis of individuals with right precordial ST-segment-elevation brugada syndrome. Circulation 2005;111:257-263.

6. Chen Q, Kirsch GE, Zhang D, Brugada R, Brugada J, Brugada P, Potenza D, Moya A, Borggrefe M, Breithardt G, Ortiz-Lopez R, Wang Z, Antzelevitch C, O'Brien RE, Schulze-Bahr E, Keating MT, Towbin JA, Wang Q: Genetic basis and molecular mechanisms for idiopathic ventricular fibrillation. Nature 1998;392:293-296.

7. Shimizu W, Aiba T, Kamakura S: Mechanisms of disease: Current understanding and future challenges in Brugada syndrome. Nat Clin Pract Cardiovasc Med 2005;2:408-414.

8. Shimizu W: Editorial comment, gender difference and drug challenge in Brugada syndrome. J Cardiovasc Electrophysiol 2004;15:70-71.

9. Di Diego JM, Cordeiro JM, Goodrow RJ, Fish JM, Zygmunt AC, Perez GJ, Scornik FS, Antzelevitch C: Ionic and cellular basis for the predominance of the Brugada syndrome phenotype in males. Circulation 2002;106:2004-2011.

10. Shuba YM, Degtiar VE, Osipenko VN, Naidenov VG, Woosley RL: Testosterone-mediated modulation of HERG blockade by proarrhythmic agents. Biochem Pharmacol 2001;62:41-49.

11. Liu XK, Katchman A, Whitfield BH, Wan G, Janowski EM, Woosley RL, Ebert SN: In vivo androgen treatment shortens the QT interval and increases the densities of inward and delayed rectifier potassium currents in orchiectomized male rabbits. Cardiovasc Res 2003;57:28-36.

12. Bai CX, Kurokawa J, Tamagawa M, Nakaya H, Furukawa T: Non-transcriptional regulation of cardiac repolarization currents by testosterone. Circulation 2005;112:1701-1710.

13. Glass AR, Swerdloff RS, Bray GA, Dahms WT, Atkinson RL: Low serum testosterone and sex-hormone-binding-globulin in massively obese men. J Clin Endocrinol Metab 1977;45:1211-1219.

14. Marin P, Holmang S, Jonsson L, Sjostrom L, Kvist H, Holm G, Lindstedt G, Bjorntorp P: The effects of testosterone treatment on body composition and metabolism in middle-aged obese men. Int J Obes Relat Metab Disord 1992;16:991-997.

15. Tsai EC, Boyko EJ, Leonetti DL, Fujimoto WY: Low serum testosterone level as a predictor of increased visceral fat in Japanese-American men. Int J Obes Relat Metab Disord 2000;24:485-491.

16. Matsuo K, Akahoshi M, Nakashima E, Seto S, Yano K: Clinical characteristics of subjects with the Brugada-type electrocardiogram: A case control study. J Cardiovasc Electrophysiol 2004;15:653-657.

17. Wilde AA, Antzelevitch C, Borggrefe M, Brugada J, Brugada R, Brugada P, Corrado D, Hauer RN, Kass RS, Nademanee K, Priori SG,

Towbin JA: Study group on the molecular basis of arrhythmias of the European Society of Cardiology. Proposed diagnostic criteria for the Brugada syndrome: Consensus report. Circulation 2002;106:2514-2519.

18. Shimizu W, Matsuo K, Takagi M, Tanabe Y, Aiba T, Taguchi A, Suyama K, Kurita T, Aihara N, Kamakura S: Body surface distribution and response to drugs of ST segment elevation in the Brugada syndrome: Clinical implication of 87-leads body surface potential mapping and its application to 12-leads electrocardiograms. J Cardiovasc Electrophysiol 2000;11:396-404.

19. Kanda M, Shimizu W, Matsuo K, Nagaya N, Taguchi A, Suyama K, Kurita T, Aihara N, Kamakura S: Electrophysiologic characteristics and implication of induced ventricular fibrillation in symptomatic patients with Brugada syndrome. J Am Coll Cardiol 2002;39:1799-1805.

20. Yokokawa M, Takaki H, Noda T, Satomi K, Suyama K, Kurita T, Kamakura S, Shimizu W: Spatial distribution of repolarization and depolarization abnormalities evaluated by body surface potential mapping in patients with Brugada syndrome. Pacing Clin Electrophysiol 2006;29:1112-1121.

21. Matsuo K, Akahoshi M, Seto S, Yano K: Disappearance of the Brugada-type electrocardiogram after surgical castration: A role for testosterone and an explanation for the male preponderance. Pacing Clin Electrophysiol 2003;26:1551-1553.

22. Litovsky SH, Antzelevitch C: Transient outward current prominent in canine ventricular epicardium but not endocardium. Circ Res 1988;62:116-126.

23. Furukawa T, Myerburg RJ, Furukawa N, Bassett AL, Kimura S: Differences in transient outward currents of feline endocardial and epicardial myocytes. Circ Res 1990;67:1287-1291.

24. Yan GX, Antzelevitch C: Cellular basis for the Brugada syndrome and other mechanisms of arrhythmogenesis associated with ST segment elevation. Circulation 1999;100:1660-1666.

25. Mok NS, Priori SG, Napolitano C, Chan NY, Chahine M, Baroudi G: A newly characterized SCN5A mutation underlying Brugada syndrome unmasked by hyperthermia. J Cardiovasc Electrophysiol 2003;14:407-411.

26. Song M, Helguera G, Eghbali M, Zhu N, Zarei MM, Olcese R, Toro L, Stefani E: Remodeling of Kv4.3 potassium channel gene expression under the control of sex hormones. J Biol Chem 2001;276:31883-31890.

27. Wickenden AD, Kaprielian R, You XM, Backx PH: The thyroid hormone analog DITPA restores I(to) in rats after myocardial infarction. Am J Physiol Heart Circ Physiol 2000;278:H1105-H1116.

28. Sunagawa M, Yamakawa M, Shimabukuro M, Higa N, Takasu N, Kosugi T: Electrophysiologic characteristics of atrial myocytes in levothyroxine-treated rats. Thyroid 2005;15:3-11.

29. Shimizu W: Acquired forms of Brugada syndrome (Antzelevitch C review). In: *The Brugada Syndrome: From Bench to Bedside*, Chapter 14. Blackwell Futura, UK, 2004:166-177.

30. Myers GB: Other QRS-T patterns that may be mistaken for myocardial infarction. IV. Alterations in blood potassium: myocardial ischemia: subepicardial myocarditis: distortion associated with arrhythmias. Circulation 1950;2:75-93.

31. Collins S, Kuhn CM, Petro AE, Swick AG, Chrunyk BA, Surwit RS: Role of leptin in fat regulation. Nature 1996;380:677.

32. Nagaya N, Moriya J, Yasumura Y, Uematsu M, Ono F, Shimizu W, Ueno K, Kitakaze M, Miyatake K, Kangawa K: Effects of ghrelin administration on left ventricular function, exercise capacity, and muscle wasting in patients with chronic heart failure. Circulation 2004;110:3674-3679.

Mechanism and New Findings in Brugada Syndrome

Wataru Shimizu, MD; Takeshi Aiba, MD; Shiro Kamakura, MD

Brugada syndrome is a clinical entity characterized by coved type ST-segment elevation in the right precordial electrocardiographic leads (V1-3) and an episode of ventricular fibrillation in the absence of structural heart disease. Although a number of clinical and experimental reports have elucidated the electrocardiographic, electrophysiologic, cellular, and molecular aspects, several problems remain unsolved. Recently developed high-resolution optical mapping techniques in arterially-perfused wedge preparations enable recording of transmembrane action potentials from 256 sites simultaneously at the epicardial surface, thus providing further advances in the understanding of the cellular mechanism of the specific ST-segment elevation and subsequent ventricular arrhythmias. In this review article, new findings relating to several unresolved problems such as gender difference (male predominance) and ethnic difference (higher incidence in Asian population) are also presented. (*Circ J* 2007; Suppl A: 000–000)

Key Words: Brugada syndrome; Ethnicity; Gender; Genetics; Mutation; Polymorphism; ST-segment; Ventricular fibrillation

rugada syndrome (BS) is characterized by coved-type ST-segment elevation in the right precordial electrocardiography (ECG) leads (V1-3) and an episode of ventricular fibrillation (VF) in the absence of acute ischemia, electrolyte abnormalities or structural heart disease.[1-8] A type-1 ST-segment elevation, which is defined as a coved ST-segment elevation of ≥0.2 mV at the J point with or without a terminal negative T wave, is required to diagnose BS, regardless of the absence or presence of sodium-channel blockers (Figs 1A,B).[7] A type-1 ST-segment elevation recorded only in the higher V1-2 leads (ie, 3rd and 2nd intercostal spaces) has been suggested to show similar prognostic value for subsequent cardiac events as that recorded in the standard V1-2 leads (Fig 1C).[7,9,10] A type-2 saddle-back ST-segment elevation alone is not diagnostic for BS (Fig 1B). The prevalence of this syndrome is estimated to be 5 per 10,000 inhabitants, and is one of the important causes of sudden cardiac death of middle-aged males in Asian countries particularly.[11,12] BS usually manifests during adulthood, with a mean age of sudden death of 41±15 years, and child cases are rare.[7] A family history of unexplained sudden death is present in approximately 20–40% of the population in Western countries, and less (15–20%) in Japan.[4,7,13,14] A significant male predominance in BS has long been reported, and more than 80% of patients in Western countries and more than 90% of patients in Asian countries affected with BS are men.[15] Since Brugada and Brugada described 8 patients with a history of aborted sudden cardiac death caused by VF as a distinct clinical entity in 1992,[1] a number of clinical and experimental reports from around the world have demonstrated the clinical, electrocardiographic, electrophysiologic, cellular, ionic, genetic and molecular features of BS.[2-14] However, several problems remain unsolved, such as genetic heterogeneity, late onset of first cardiac events, and gender and ethnic differences.[8] In this review article, we present our recent data relating to the cellular and molecular mechanism of BS, the late onset of its clinical manifestation, male predominance, and higher incidence in Asian populations.

Genetic and Molecular Aspects

Advances in molecular genetics in the past decade have established a link between several inherited cardiac arrhythmias, including BS and long QT syndrome, and mutations in genes encoding ion channels, membrane components or receptors.[16] In 1998, the first mutation linked to BS was identified by Chen et al in *SCN5A*,[17] the gene encoding the α subunit of the sodium channel. Thereafter, a large family of BS was reported to link to a second locus on chromosome 3, which is close to but different from the *SCN5A* locus;[18] however, specific gene or genes other than *SCN5A* have not yet been identified on chromosome 3. *SCN5A* mutations are reported to account for 18–30% of clinically diagnosed BS patients at present.[7] Antzelevitch et al have recently reported that 3 probands associated with a BS-like ST-segment elevation and a short QT interval were linked to mutations in *CACNA1C* (A39V and G490R) or *CACNB2* (S481L), the gene encoding the α1 or β2b subunit of the L-type calcium channel, respectively.[19] Their genetic and heterologous expression studies revealed loss of function of the L-type calcium channel current (I$_{Ca-L}$). However, approximately two-thirds of BS patients have not been yet genotyped, suggesting the presence of genetic heterogeneity.[8] Other candidate genes for the Brugada phenotype include those encoding the transient outward current (I$_{to}$) and the delayed rectifier potassium current (I$_K$), or those coding the adrenergic receptors, cholinergic receptors, ion-channel-interacting protein, promoters, transcriptional factors, neurotransmitters, or transporters.[7,8]

Among the approximately 100 mutations in *SCN5A* linked to BS, more than 24 of them have been studied in expression systems, and have been shown to result in loss of function of the sodium channel current (I$_{Na}$) by several
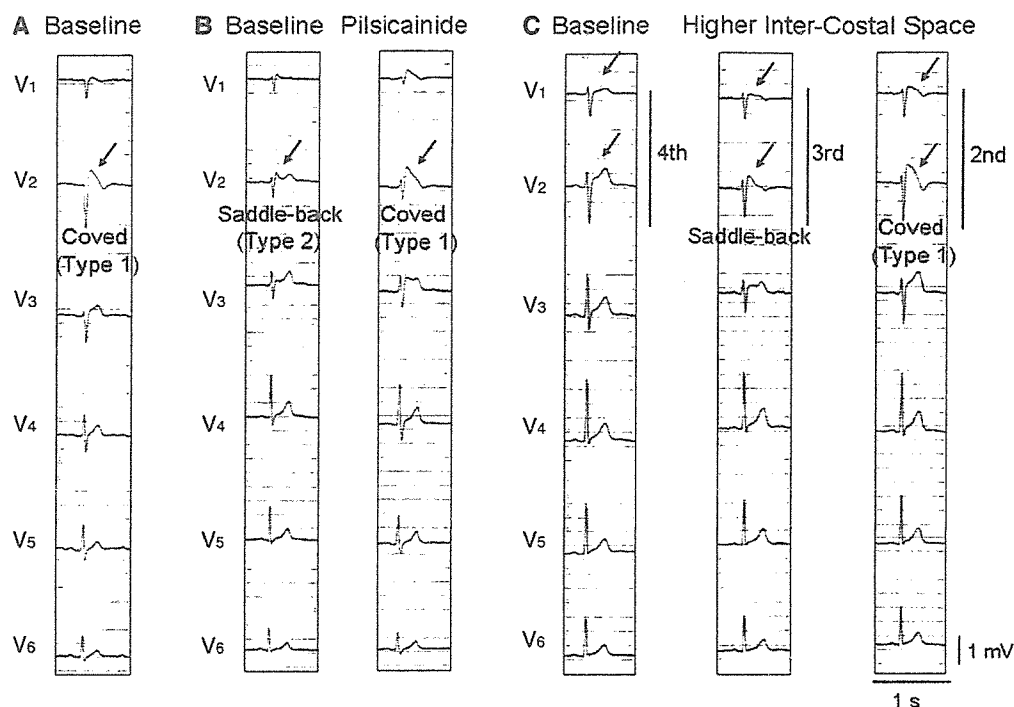
Fig 1.   (A) Spontaneous type 1 coved type ST-segment elevation (arrow). (B) Unmasking of ST-segment elevation by a class IC sodium-channel blocker, pilsicainide. Under baseline conditions, type 2 saddle-back type ST-segment elevation is recorded in lead V2 (Left, arrow). Pilsicainide injection (30 mg) unmasks the type 1 coved type ST-segment elevation in lead V2 (Right, arrow). (C) Unmasking of the type 1 electrocardiogram (ECG) by recording the right precordial (V1-2) leads at the 3rd and 2nd intercostal spaces. No significant ST-segment elevation is observed in leads V1 and V2 of the standard 12-lead ECG (4th intercostal space) (Left, arrow), whereas saddle-back type (Middle, arrow) and type 1 coved type (Right, arrow) ST-segment elevation are unmasked in leads V1 and V2 recorded from the 3rd and 2nd intercostal spaces, respectively.

mechanisms[20] These functional effects include: (1) lack of expression of the sodium channel; (2) a shift in the voltage-dependence and time-dependence of I_{Na} activation, inactivation or reactivation; (3) entry of the sodium channel into an intermediate state of inactivation from which it recovers more slowly; (4) accelerated inactivation of the sodium channel; and (5) a trafficking defect. Some common *SCN5A* polymorphisms are reported to modulate the functional consequences of primary *SCN5A* mutations. Baroudi et al first suggested that the interaction of *SCN5A* polymorphisms and *SCN5A* mutations may affect the consequence of the functional effects. They reported that a common polymorphism (R1232W) of *SCN5A* affected protein trafficking when it was co-expressed with a T1620M mutation, although the T1620M mutation alone produced only gating abnormalities in the I_{Na}[21] On the other hand, another common polymorphism (H558R) of *SCN5A* was reported by Ye et al to rescue normal trafficking and normal I_{Na} for the M1766L mutant protein[22] These effects of common *SCN5A* polymorphisms on modifying the functional consequence of *SCN5A* mutations may make the clinical phenotype more complex.

Cellular Mechanism of Brugada Phenotype

The I_{to}-mediated phase 1 notch of the action potential (AP) has been reported to be larger in the epicardium than in the endocardium in many species, including humans[23] Because the maintenance of the AP dome is determined by the fine balance of currents active at the end of phase 1 of the AP (principally I_{to} and I_{Ca-L}), any interventions that cause a

net outward shift in the current active at the end of phase 1 can increase the magnitude of the AP notch, leading to loss of the AP dome (all-or-none repolarization) in the epicardium, but not in the endocardium, contributing to a significant voltage gradient across the ventricular wall during ventricular activation[23] The heterogeneous loss of the AP dome in the epicardium has been shown to produce premature beats via a mechanism of phase 2 reentry in experimental studies using isolated sheets of canine right ventricle[24] Therefore, these mechanism of all-or-none repolarization in the epicardial cells and phase 2 reentry-induced premature beat between the adjacent epicardial cells were expected to be responsible for the clinical phenotype in BS.

In the late 1990s, Antzelevitch's group developed an experimental model of BS using arterially perfused canine right ventricular (RV) wedge preparations, in which transmembrane APs and pseudo-ECGs were simultaneously recorded. These experimental studies have provided significant insights of the cellular mechanism of the Brugada phenotype, ST-segment elevation and subsequent VF[25,26] The I_{to}-mediated AP notch and the loss of the AP dome in the epicardial cells, but not in the endocardial cells, of the right ventricle gives rise to a transmural voltage gradient, producing ST-segment elevation in the ECG in the wedge preparations. Fig 2 shows transmembrane APs simultaneously recorded from 2 epicardial (Epi) and 1 endocardial sites, together with a transmural ECG in a Brugada model using the RV wedge preparation. Under control conditions, a small J wave coincides with the small notch observed in the epicardial cells, but not in the endocardial cells (Fig 2A). Combined administration of terfenadine (I_{Ca-L} block) and
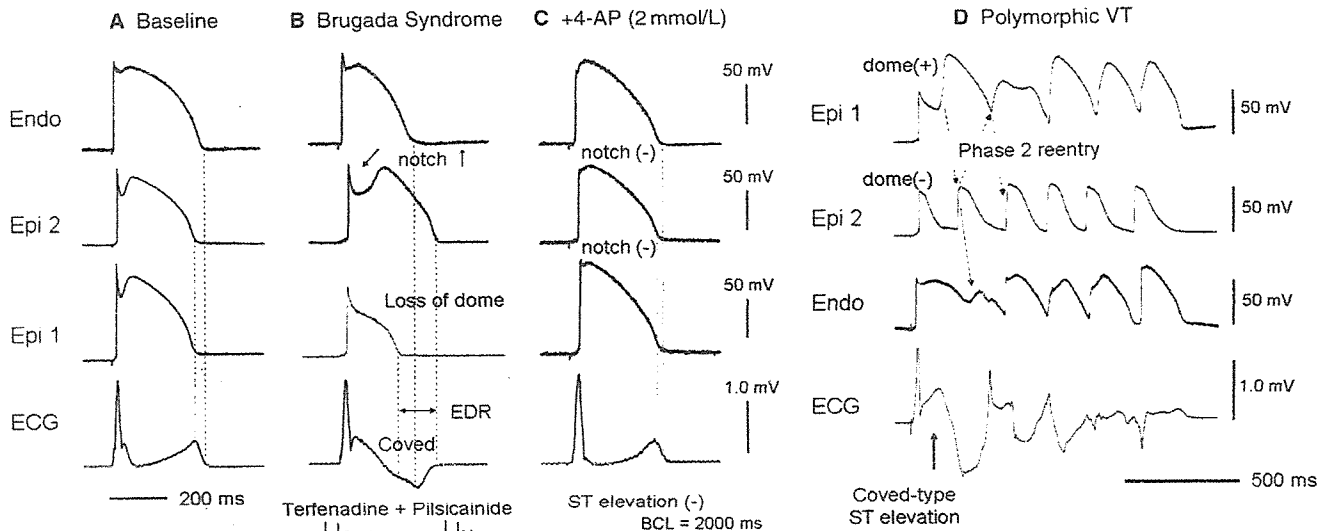
Fig2. Type 1 coved type ST-segment elevation and non-sustained polymorphic ventricular tachycardia (VT) via phase 2 reentry induced in a Brugada model using an arterially perfused canine right ventricular wedge preparation. Shown are transmembrane action potentials (APs) simultaneously recorded from 2 epicardial sites (Epi 1 and Epi 2) and 1 endocardial site (Endo) together with a transmural ECG (basic cycle length (BCL)=2,000 ms). (A) Under baseline conditions, phase 1 AP notch in Epi, but not in Endo, is associated with a J wave in the ECG. (B) Combined administration of terfenadine (5 μmol/L) and pilsicainide (5 μmol/L) produces a loss of AP dome in Epi 1, but not in Epi 2, resulting in a marked epicardial dispersion of repolarization (EDR), and a coved-type ST segment elevation and a negative T wave in the ECG. (C) 4-aminopyridine (4-AP), a selective blocker of the transient outward current (I_{to}) (2 μmol/L), restores the AP dome, decreases the phase 1 AP notch, and normalizes the ST-segment elevation. (D) In the setting of heterogeneous loss of the AP dome (coexistence of loss of dome regions and restored dome regions) in the epicardium and a remarkable coved type ST-segment elevation in the ECG with combined administration with terfenadine and pilsicainide, electrotonic propagation from the site where the dome is restored (Epi 1) to the site where it is lost (Epi 2) results in development of a premature beat induced by phase 2 reentry, triggering spontaneous polymorphic VT (Modified from *Nat Clin Pract Cardiovasc Med* 2005; **2**: 408–414 with permission).

pilsicainide (I_{Na} block) produces a loss of the AP dome in Epi 1, but not in Epi 2, resulting in a marked epicardial dispersion of repolarization (EDR), and a coved-type ST segment elevation and negative T wave in the ECG (Fig 2B). A selective I_{to} blocker, 4-aminopyridine, restores the AP dome, decreases the phase 1 AP notch, and normalizes the ST-segment elevation (Fig 2C). Fig 2D shows non-sustained polymorphic ventricular tachycardia (VT) via phase 2 reentry induced in a Brugada model using the wedge preparation. In the setting of remarkable coved type ST-segment elevation with combined administration of terfenadine and pilsicainide, heterogeneous loss of the AP dome (coexistence of loss of dome regions and restored dome regions) in the epicardium creates a marked EDR, giving rise to premature beats caused by phase 2 reentry, which precipitates non-sustained polymorphic VT.

Optical Mapping Study

The AP data in the Brugada model using arterially perfused canine RV wedge preparations strongly supported the hypothesis that episodes of VF in BS are triggered by premature beats between the adjacent epicardial cells via the mechanism of phase 2 reentry. However, the precise mechanism of the initial premature beats and the maintenance of non-sustained polymorphic VT or VF remain unsolved, because the number of AP recording sites available for floating microelectrodes is small in the wedge preparations. To overcome this limitation, we recently developed high-resolution (256×256) optical mapping techniques that allowed us to record transmembrane APs from 256 sites

simultaneously at the epicardial or endocardial surface of the wedge preparations (Figs 3–5)[8,27] Fig 3 shows the mechanism of phase 2 reentry-induced premature beats (P2R-extrasystoles) under Brugada-ECG conditions. A steep repolarization gradient between the loss of dome region and the restored dome region in the epicardium, but not in the endocardium, develops the initial P2R-extrasystole. We then recorded spontaneous episodes of P2R-extrasystoles and subsequent non-sustained polymorphic VT or VF under these conditions, and analyzed the epicardial AP duration (APD) and conduction velocity (Figs 4,5). Once again, most of the P2R-extrasystoles originated from the area showing the steepest (maximum) gradient of repolarization (GR_{max}) between the loss of dome site and the restored dome site in the epicardium (Figs 4C,5C, arrows), leading to non-sustained polymorphic VT or VF. These data also indicate that a steep repolarization gradient between the loss of dome region and the restored dome region in the epicardium is essential to produce the P2R-extrasystoles that precipitate polymorphic VT or VF. On the other hand, the epicardial GR_{max} does not differ between episodes of polymorphic VT and those of VF. Figs 4D,E and 5D,E show the mechanism underlying the difference between polymorphic VT and VF. Just before inducing the episodes of polymorphic VT or VF, the epicardial depolarization map paced from the endocardium at the basic cycle length of 2,000 ms shows a remarkable conduction delay in the episode of VF (Fig 5D) compared with that of polymorphic VT (Fig 4D). The conduction parameters, such as QRS duration and interval between the stimulus and the earliest epicardial activation, are significantly longer in the epi-